International Journal of Nanoscience
Vol. 14, Nos. 1 & 2 (2015) 1460027 (6 pages)

DOI: 10.1142/S0219581X14600278

World Scientific
www.worldscientific.com

Electrochemical Behavior of $LiFePO_4$ Thin Film Prepared by RF Magnetron Sputtering in Li_2SO_4 Aqueous Electrolyte

Jiaxiong Wu*, Wei Cai and Guangyi Shang†
Department of Applied Physics, Beihang University, Beijing 100191, P. R. China
Key Laboratory of Micro-Nano Measurement Manipulation and Physics (Ministry of Education), Beihang University, Beijing 100191, China
*jxwu@buaa.edu.cn
†gyshang@buaa.edu.cn

Received 29 September 2014
Accepted 16 October 2014
Published 12 January 2015

$LiFePO_4$ films were deposited on Au/Si substrate by radio-frequency magnetron sputtering. The effect of annealing on the crystallization and morphology of $LiFePO_4$ thin film has been investigated. X-ray diffraction revealed that the films through annealing were well crystallized compared with as-deposited films. The surface morphology of the thin film was also observed by scanning electron microscopy (SEM) and atomic force microscopy (AFM). Electrochemical tests in 1M Li_2SO_4 showed that the annealed thin film in 500°C exhibits larger Li-ion diffusion coefficient ($3.46 \times 10^{-7}\,cm^2s^{-1}$) than as-deposited film and powder. Furthermore, cyclic voltammetry demonstrate a well-defined lithium intercalation/deintercalation reaction at around 0.45 V versus SCE (i.e., 3.6 V versus Li^+/Li), suggesting that the annealed $LiFePO_4$ thin film is a promising candidate cathode film for lithium microbatteries.

Keywords: $LiFePO_4$ thin film; aqueous rechargeable lithium-ion microbatteries; magnetron sputtering.

1. Introduction

With the depletion of traditional energy and environment problems caused by coal or oil, the development of new energy sources has been becoming more and more important. Li-ion battery is one of new sources and has been widely used in kinds of electronic devices in our daily life.[1] Padhi first introduced lithium iron phosphate ($LiFePO_4$) as a cathode material.[2] It has been considered as the most promising candidate electrode material because it has high theoretical specific capacity ($170\,mAhg^{-1}$) and thermal stability under high temperature.[3] Unfortunately, $LiFePO_4$ suffers low electronic conductivity and slow lithium ion diffusion coefficient.[4] These problems are able to be solved by means of thin film technology, because the thickness of cathode material can be greatly reduced. In the case the poor electronic conductivity does not affect the electrochemical performance of electrode.[5,6] $LiFePO_4$ thin film electrodes have been

successfully prepared by radio frequency magnetron sputtering. The composition, morphology and thickness of thin film are very sensitive to temperature of substrate.[7,8] The electrochemical performance of the film in non-aqueous electrolyte has been researched. Li-ion chemical diffusion coefficients (D_{Li}) vary with thickness of thin film. Thicker film shows larger D_{Li} values than thinner film.[9,10] The cycling capacity of $LiFePO_4$ film suffer a big decrease in Li-ion micro-batteries.[11,12] The 1 μm thick film of $LiFePO_4$ can deliver over 150 $mAhg^{-1}$ at discharge current of 1C, and the capacity will retain only 50% at 2C.[13]

As we know, organic liquid is generally used as electrolyte in a traditional Li-ion battery. Drawbacks of organic electrolyte are obvious, such as the safety and environment problems.[14] When battery is retirement, electrolyte may leak into the land and cause land contamination.[15,16] In addition, nonaqueous electrolytes make the manufacturing process of battery more complicated and expensive. Because of these obvious disadvantages, the development of more efficient and environment-friendly battery is necessary, for example, aqueous rechargeable Li-ion battery (ARLB).[17] Actually, with the development of electrochemical energy-storage devices using aqueous electrolytes, research work on different compounds in aqueous electrolyte, such as $LiMn_2O_4$,[18,19] $LiCoO_2$,[20] especially $LiFePO_4$[21–23] have attracted more attention to study their fundamental performance in aqueous electrolyte. However, little work on the film electrode that is used in Li-ion microbatteries published up-to now.

In this paper, we focus on the preparation and electrochemical behavior of $LiFePO_4$ thin film. The synthesized method of $LiFePO_4$ thin film electrode using the radio frequency magnetron sputtering deposition was developed. The effect of annealing on the crystallization and morphology of the thin film were studied. The Li-ion diffusion coefficient and electrochemical behavior in 1M Li_2SO_4 aqueous electrolyte were investigated.

2. Experiment

$LiFePO_4$ films were deposited on Si substrate by rf magnetron sputtering using a 2 in. target. $LiFePO_4$ powder was prepared by solid-state reactions with stoichiometric Li_2CO_3, $FeC_2O_4 \cdot 2H_2O$ and $(NH_4)_2HPO_4$ at 500°C for 3 h. The $LiFePO_4$ powder was then cold pressed and sintered again at 750°C under Ar/H_2 (2% H_2) atmosphere for 24 h to obtain 2 in. diameter $LiFePO_4$ target.

The $LiFePO_4$ target was sputtered in flowing Ar (purity 99.99%) at a pressure of 2.7 Pa, and the flow rate was 50 standard cm^3/min (sccm). An rf magnetron sputtering power of 70 W was applied to the target. The distance between the target and the substrate was 5 cm. Before deposition of the $LiFePO_4$ films, the target and the substrate are presputtered under identical conditions in order to eliminate contaminants atoms from the surface of target and substrate. The temperature of substrate during deposition is range from 25°C to 300°C. The as-prepared thin film was annealed at 500°C for 2 h to increase the crystallization degree.

The crystal structure of the $LiFePO_4$ powder and thin film were characterized by X-ray diffraction with CuKα1 radiation source filtered by Ni film operated at a voltage of 40 KV at a scan speed of 5°/min in the range 15–40°C. The surface morphology of thin films was characterized by field-emission scanning electron microscopy (FE-SEM, JEOL, S-4800) and atomic force microscopy (AFM, CSPM).

Electrochemical properties of $LiFePO_4$ and its film electrodes were studied by a standard three-electrode cell. $LiFePO_4$ electrode was prepared as following procedure: stoichiometric LiFePO4 powder, PVDF and super P carbon were dissolved in N-methylpyrrolidone (NMP). The suspension was stirred for 1 h. Subsequently, the suspension was coated on a platinum foil and dried at 80°C for 6 h. The reference electrode was a saturated calomel electrode (SCE, E = 0.245 V versus standard hydrogen electrode, NHE). Platinum plate was used as counter electrode. The electrolyte was 1M Li_2SO_4 aqueous solution. Cyclic voltammetry measurement was performed in the range of −0.8 V to 1.0 V safe voltage window without H_2O decomposition.[24] All the cyclic voltammetry experiments were carried on a CHI600D electrochemical working station. All potentials were measured with respect to saturated calomel electrode. The electrochemical experiments were performed under ambient temperature.

3. Results and Discussion

3.1. *Crystallography*

The XRD patterns of $LiFePO_4$ target and thin film deposited on Si substrate followed by annealing are shown in Fig. 1. It can be seen from the Fig. 1(b)

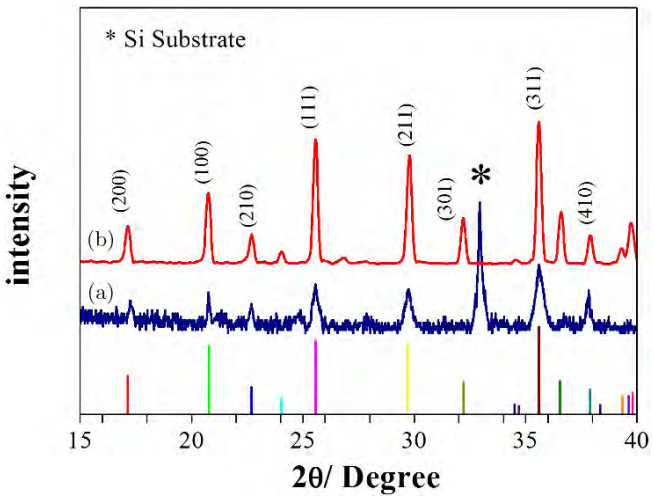

Fig. 1. X-ray diffraction pattern of $LiFePO_4$. (a) $LiFePO_4$ film deposited in 300°C following annealing at 500°C and (b) $LiFePO_4$ target powder.

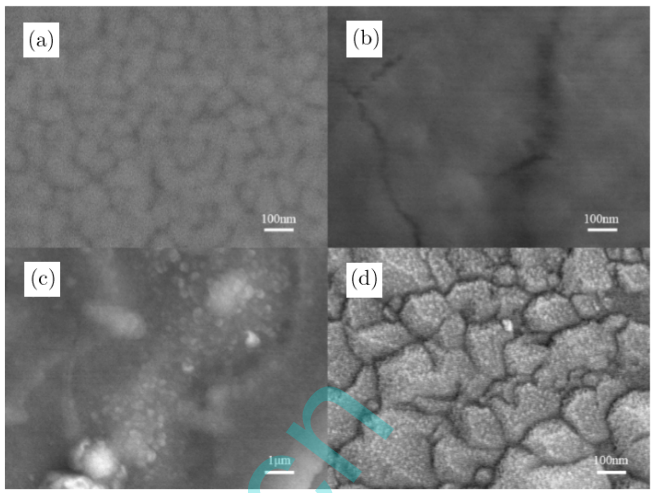

Fig. 2. SEM surface morphology of $LiFePO_4$ film deposited in (a) 25°C, (b) 200°C, (c) 300°C and (d) annealing at 500°C.

that the powder scraped from the target exhibit a single phase formation of an olivine structure, which indicates that sample is well indexed to an orthorhombic crystal structure with Pnmb space group (JCDPS Card No. 81-1173) without any impurity phase. The lattice parameters are determined by the least squares method from Pnmb orthorhombic space group. The calculated lattice parameters are $a = 10.29$ Å, $b = 5.99$ Å, $c = 4.65$ Å which are in good agreement with theoretical parameters.

The XRD patterns of as-deposited $LiFePO_4$ thin films at 25°C, 200°C and 300°C show amorphous pattern. There is a strongest reflection peak in 33° which is identified the Si substrate. As the annealing temperature increased to 500°C for 4 h, the film deposited at 300°C shows a crystallized and predominant $LiFePO_4$ phase, in which (311) is the strongest reflection peak as shown in Fig. 1(a). However, the intensity ratios of film X-ray peaks are slightly different from the powder target and there are some slight amounts of impurities. This is due to the target oxidation in plasma by the residual O_2 and H_2O vapor in the chamber.

3.2. *Surface morphology*

Figures 2 and 3 show the surface morphology of deposited films on Si substrate observed by SEM and AFM. Figure 2 shows that the as-deposited films at 25°C, 200°C and 300°C has no obvious grains and boundaries in surface, which consistent with the X-ray amorphous pattern. Through the annealing process at temperature of 500°C, it is found that the film surface is composed of crystallized particles in Fig. 2(d). The size of particles is 200 nm with apparently grain boundaries. The morphology change of film from amorphous to uniformity is due to the fact that high annealing temperature promotes continuous grain growth. Representative AFM images of the bare film are shown in Fig. 3. The height and deflection images of as-deposited film at 25°C, 200°C and 300°C show amorphous pattern without obvious particles and grain boundaries in Figs. 3(a)–3(c). The result is consistent with these of SEM and X-ray pattern shown in Figs. 1 and 2. In contrast, it can be seen apparently grain boundaries from height and deflection image of the annealed films in Fig. 3(d) which are detected under atmosphere. The results obtained with the AFM are in agreement with these taken with the SEM.

3.3. *Electrochemical tests*

The electrochemical performance of $LiFePO_4$ powder and deposited film are characterized by cyclic voltammetry. CVs are recorded in the voltage range of −0.8 V to 1.2 V at various scan rates and the best CV results at 1 mV/s were obtained, using a three electrode system, which has been described in detail in experimental section. Figure 4 presents a typical first cyclic voltammetry curve for both powder and film prepared in our study. It shows very clearly one pair of well-defined and symmetrical redox peaks for

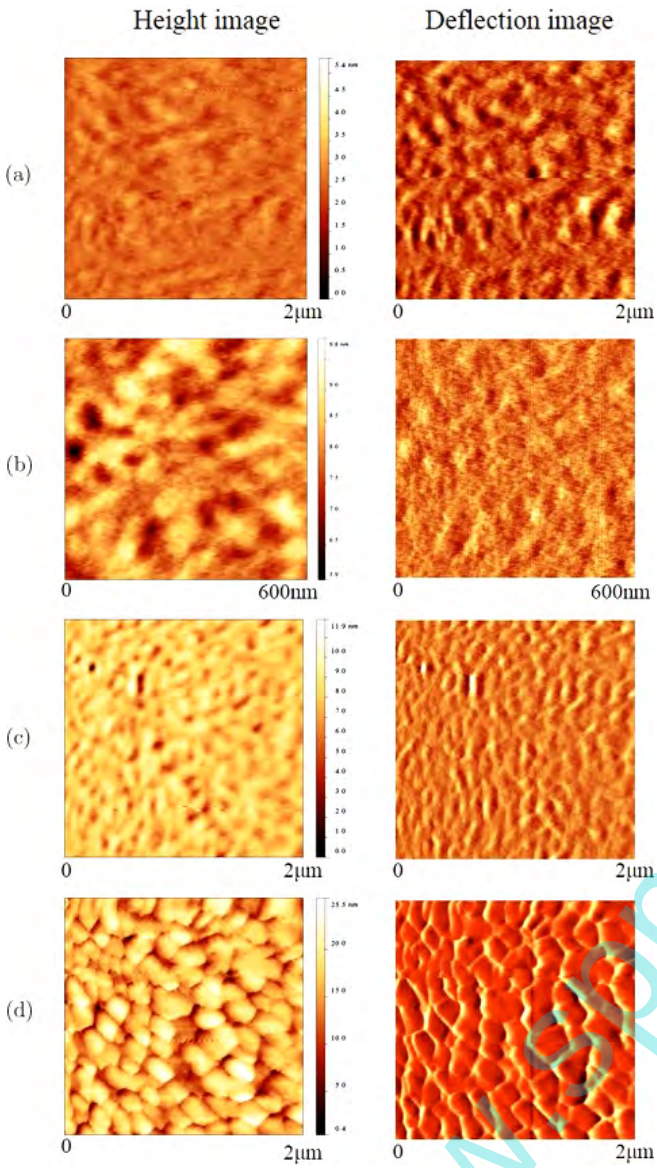

Fig. 3. AFM surface morphology of $LiFePO_4$ film deposited in (a) 25°C, (b) 200°C, (c) 300°C and (d) annealing at 500°C.

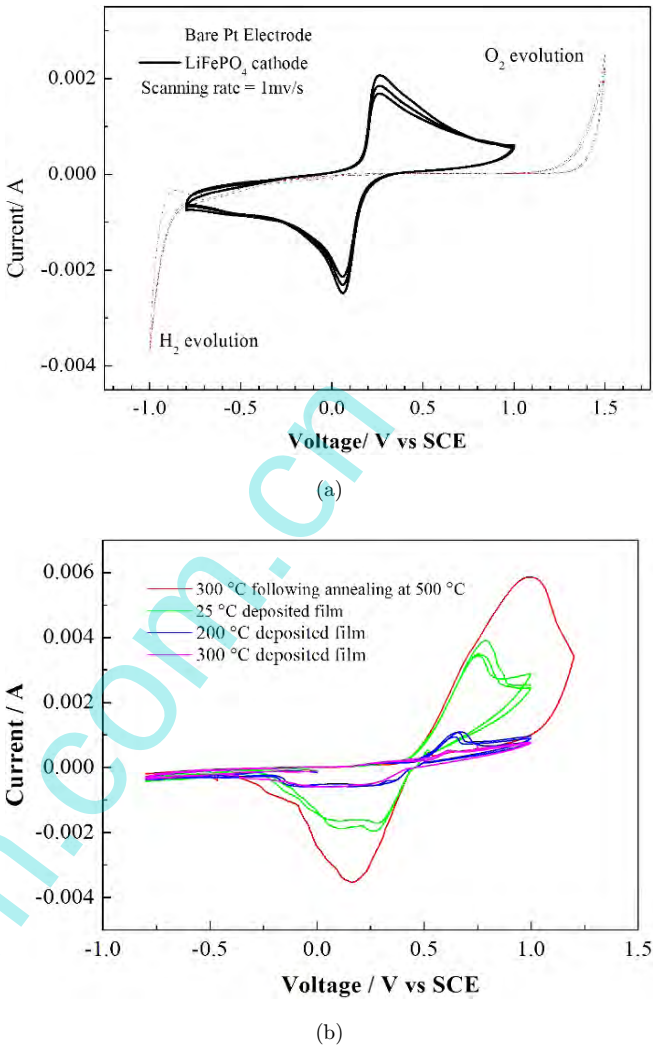

Fig. 4. (a) Cyclic voltammetry of $LiFePO_4$ powder in 1M Li_2SO_4 aqueous electrolyte and (b) cyclic voltammetry of $LiFePO_4$ thin film in 1M Li_2SO_4 aqueous electrolyte.

$LiFePO_4$ electrode. The appearance of this pair redox peaks can be explained based on redox activity of iron species in $LiFePO_4$. Therefore, the anodic peak appears to be the oxidation of Fe^{2+} to Fe^{3+} while the cathodic peak due to the reduction of Fe^{3+} to Fe^{2+}. The redox process in 1M Li_2SO_4 electrolyte is accompanied with Li ion insertion and de-insertion has been discussed.

The peak currents I_p during anodic scans are applied to extract the Li-ion diffusion coefficient D, utilizing the Randles–Sevick equation:

$$I_p = 2.69 \times 10^5 ACD^{1/2} n^{3/2} \nu^{1/2} \quad (1)$$

where A is the electrode area, C is the shuttle concentration, n is the number of electrons involved in the redox process ($n = 1$, for Fe^2/Fe^{3+} redox pair) and ν is the potential scan rate. Utilizing these data, we can obtain the Li-ion diffusion coefficients of the $LiFePO_4$ powder, 25°C, 200°C, 300°C deposited film and annealed film at 500°C. The value have been calculated to be 5.53×10^{-8}, 3.45×10^{-9}, 1.05×10^{-7} and $3.46 \times 10^{-7}\,cm^2s^{-1}$, respectively. It is obvious that the 300°C deposited film following annealing at 500°C owned larger D_{Li} than powder and as-deposited film. This is due to the film increase the electrochemical performance and regular crystalic structure of the annealed film.

The CV curve indicate that the redox reaction mechanism of $LiFePO_4$ in Li_2SO_4 aqueous electrolyte is similar to that in non-aqueous electrolyte. As

we know, the corresponding equations of the redox reactions represented by peaks of $LiFePO_4$ in Fig. 4 can be written as

Oxidation:

$$LiFePO_4 - xLi^+ - xe^- \rightarrow xFePO_4 + (1-x)LiFePO_4 \quad (2)$$

Reduction:

$$FePO_4 + xLi + xe^- \rightarrow xLiFePO_4 + (1-x)FePO_4 \quad (3)$$

The formal potential (E_f) can be calculated from anodic/cathodic peak potential based on the equation:

$$E_f = \frac{E_a + E_c}{2} \quad (4)$$

It can be seen from Fig. 4(a) that lithium deintercalation and intercalation potential in aqueous are 0.28 V and 0.08 V versus SCE, respectively. The corresponding voltage versus Li^+/Li can be calculated: 3.57 V and 3.36 V versus Li^+/Li. Therefore, the calculated E_f value will be 3.47 V versus Li^+/Li which is slightly different from the theoretical value of 3.5 V versus Li^+/Li. This difference is possibly due to the structure and morphology that affect the electrochemistry of $LiFePO_4$.

Figure 4(b) shows the CV result of as-deposited and annealed $LiFePO_4$ films. There hardly have redox peaks recorded for the film deposited at 25°C and 200°C because the current is so small. In contrast, sharp and typical redox are exhibited for the film which deposited in 300°C following annealing at 500°C. The ratio between anodic and cathodic peak current is close to 1, show a good reversibility of lithium ion intercalation into and deintercalation from annealed films. The result could be attributed to the crystallites of the annealed films. It is obvious that finer grains have larger active surface and higher electrochemical reactivity, which promote the Li-ion diffusion and widen the redox potential range. The CV curves shows an anodic peak occurring at 0.75 V versus SCE and a cathodic peak occurring at 0.2 V versus SCE. It can be calculated that the formal potential is 0.45 V versus SCE, i.e., 3.6 V versus Li^+/Li, which is slightly larger than the value of powder and theoretical voltage in non-aqueous electrolyte. This is due to that the thickness of film cathode is greatly decreased so that the poor electronic conductivity cannot affect the electrochemical performance of electrode.

4. Conclusion

$LiFePO_4$ powder has been synthesized and the thin film sputtered in Si substrate using radio frequency magnetron sputtering method has been prepared. The XRD studies revealed that the film deposited at 25°C, 200°C and 300°C substrate exhibit amorphous pattern. The film prepared at 300°C following annealing at 500°C show crystallic structure and contains pure $LiFePO_4$ phase. Detailed cyclic voltammetry investigation revealed that both $LiFePO_4$ powder and annealed film undergo Li-ion intercalation/deintercalation in Li_2SO_4 aqueous electrolyte. The film deposited in 300°C following annealing at 500°C show a higher Li-ion diffusion coefficient than powder and as-deposited film. An analysis of voltage illustrates that the powder and annealed film in Li_2SO_4 aqueous electrolyte can deliver a compatible voltage compared with that in non-aqueous electrolyte. In particularly, the annealed $LiFePO_4$ film exhibit a higher voltage than powder. It is demonstrated that the annealed $LiFePO_4$ film can be used as a promising cathode film for aqueous recharge lithium microbatteries.

Acknowledgments

We are grateful for financial support from the National 973 Project (No. 2013CB934004), National Natural Science Foundation of China (NSFC) (No. 11232013 and 11304006) and Fundamental Research Funds for the Central Universities (YWF-13-D2-XX-14).

References

1. M. Armand and J.-M. Tarascon, *Nature* **451**, 652 (2008).
2. A. K. Padhi, K. S. Nanjundaswamy and J. B. Goodenough, *J. Electrochem. Soc.* **144**, 1188 (1997).
3. J. B. Goodenough and Y. Kim, *Chem. Mater.* **22**, 587 (2010).
4. A. Yamada, S. C. Chung and K. Hinokuma, *J. Electrochem. Soc.* **148**, A224 (2001).
5. K.-F. Chiu and P. Chen, *Surf. Coat. Tech.* **203**, 872 (2008).
6. J. Xie *et al.*, *Electrochim. Acta.* **54**, 4631 (2009).
7. X.-J. Zhu *et al.*, *J. Phys. Chem. C* **113**, 14518 (2009).
8. A. Yamada, S. C. Chung and K. Hinokuma, *J. Electrochem. Soc.* **148**, A224 (2001).
9. K. Tang *et al.*, *Electrochim. Acta.* **56**, 4869 (2011).
10. M. Köhler *et al.*, *J. Power Sources* **236**, 61 (2013).

11. K. F. Chiu, *J. Electrochem. Soc.* **154**, A129 (2007).
12. A. Eftekhari, *J. Electrochem. Soc.* **151**, A1816 (2004).
13. J. Hong *et al.*, *J. Electrochem. Soc.* **154**, A805 (2007).
14. S. Al-Hallaj and J. R. Selman, *J. Power Sources* **110**, 341 (2002).
15. P. Nelson *et al.*, *J. Power Sources* **110**, 437 (2002).
16. R. Spotnitz and J. Franklin, *J. Power Sources* **113**, 81 (2003).
17. X. Wang *et al.*, *Sci. Rep.* **3**, 1401 (2013).
18. N. N. Sinha *et al.*, *Int. J. Electrochem. Sci.* **3**, 691 (2008).
19. M. Jayalakshmi, M. Mohan Rao and F. Scholz, *Langmuir* **19**, 8403 (2003).
20. M. M. Rao *et al.*, *J. Solid State Electrochem.* **5**, 50 (2001).
21. P. He *et al.*, *Electrochim. Acta.* **56**, 2351 (2011).
22. M. Zhao *et al.*, *J. Power Sources* **211**, 202 (2012).
23. J.-H. Lee *et al.*, *J. Phys. Chem. C* **114**, 4466 (2010).
24. C. H. Mi, X. G. Zhang and H. L. Li, *J. Electroanal. Chem.* **602**, 245 (2007).